Pathway-Based Analysis of the Liver Response to Intravenous Methylprednisolone Administration in Rats: Acute Versus Chronic Dosing

Gene Regulation and Systems Biology
Volume 13: 1–20

DOI: 10.1177/1177625019840282

Alison Acevedo[1], Ana Berthel[2], Debra DuBois[3,4], Richard R Almon[3,4], William J Jusko[3,4] and Ioannis P Androulakis[1,5,6]

[1]Department of Biomedical Engineering, Robert Wood Johnson Medical School, Rutgers, The State University of New Jersey, Piscataway, NJ, USA. [2]Department of Biochemistry, Mount Holyoke College, South Hadley, MA, USA. [3]Department of Pharmaceutical Sciences, School of Pharmacy and Pharmaceutical Sciences, The State University of New York at Buffalo, Buffalo, NY, USA. [4]Department of Biological Sciences, The State University of New York at Buffalo, Buffalo, NY, USA. [5]Department of Chemical and Biochemical Engineering, Robert Wood Johnson Medical School, Rutgers, The State University of New Jersey, Piscataway, NJ, USA. [6]Department of Surgery, Robert Wood Johnson Medical School, Rutgers, The State University of New Jersey, Piscataway, NJ, USA.

ABSTRACT: Pharmacological time-series data, from comparative dosing studies, are critical to characterizing drug effects. Reconciling the data from multiple studies is inevitably difficult; multiple in vivo high-throughput -omics studies are necessary to capture the global and temporal effects of the drug, but these experiments, though analogous, differ in (microarray or other) platforms, time-scales, and dosing regimens and thus cannot be directly combined or compared. This investigation addresses this reconciliation issue with a meta-analysis technique aimed at assessing the intrinsic activity at the pathway level. The purpose of this is to characterize the dosing effects of methylprednisolone (MPL), a widely used anti-inflammatory and immunosuppressive corticosteroid (CS), within the liver. A multivariate decomposition approach is applied to analyze acute and chronic MPL dosing in male adrenalectomized rats and characterize the dosing-dependent differences in the dynamic response of MPL-responsive signaling and metabolic pathways. We demonstrate how to deconstruct signaling and metabolic pathways into their constituent pathway activities, activities which are scored for intrinsic pathway activity. Dosing-induced changes in the dynamics of pathway activities are compared using a model-based assessment of pathway dynamics, extending the principles of pharmacokinetics /pharmacodynamics (PKPD) to describe pathway activities. The model-based approach enabled us to hypothesize on the likely emergence (or disappearance) of indirect dosing-dependent regulatory interactions, pointing to likely mechanistic implications of dosing of MPL transcriptional regulation. Both acute and chronic MPL administration induced a strong core of activity within pathway families including the following: lipid metabolism, amino acid metabolism, carbohydrate metabolism, metabolism of cofactors and vitamins, regulation of essential organelles, and xenobiotic metabolism pathway families. Pathway activities alter between acute and chronic dosing, indicating that MPL response is dosing dependent. Furthermore, because multiple pathway activities are dominant within a single pathway, we observe that pathways cannot be defined by a single response. Instead, pathways are defined by multiple, complex, and temporally related activities corresponding to different subgroups of genes within each pathway.

KEYWORDS: omics, corticosteroids, pathway analysis, methylprednisolone, dose comparison

RECEIVED: January 14, 2019. **ACCEPTED:** March 5, 2019.

TYPE: Original Research

FUNDING: The author(s) disclosed receipt of the following financial support for the research, authorship, and/or publication of this article: This work was supported in part by the NIH Biotechnology Training Program (Award T32 GM008339), the U.S. Department of Education Graduate Assistance in Areas of National Need (GAANN; P200A150131), and the NIH GM24211.

DECLARATION OF CONFLICTING INTERESTS: The author(s) declared no potential conflicts of interest with respect to the research, authorship, and/or publication of this article.

CORRESPONDING AUTHOR: Ioannis P Androulakis, Department of Biomedical Engineering, Robert Wood Johnson Medical School, Rutgers, The State University of New Jersey, 599 Taylor Rd, Piscataway, NJ 08854, USA. Email: yannis@rci.rutgers.edu

Introduction

Synthetic glucocorticoids (GCs), such as methylprednisolone (MPL), are widely used anti-inflammatory and immunosuppressive agents for the treatment of a variety of inflammatory and auto-immune conditions.[1,2] Glucocorticoid drugs magnify the actions of endogenous GC regulating pathways by binding of a drug-receptor complex to DNA GC regulatory elements (GREs) or by signaling through receptors in a transcription-independent manner.[3] Because of the diverse effects of GC and the multitude of molecular mechanisms involved, in vivo high-throughput transcriptomics has proven effective in better understanding the temporal and tissue-specific effects of MPL.[4–12]

However, while short-term corticosteroid (CS) use is beneficial for reducing inflammation, long-term use is associated with serious consequences including hyperglycemia, negative nitrogen balance, and fat redistribution leading to complications including diabetes, muscle wasting, and osteoporosis.[13,14] Therefore, adding to the complexity of the physiological and pharmacological effects of CSs,[6,7,15] different dosing regimens of GC administration induce different patterns of expression[5,16,17] likely indicative of dosing-dependent regulation. Thus, transcriptional dynamics under acute CS administration may not exhibit similar expression patterns during continuous infusion, pointing to the possibility of alternative regulatory mechanisms.[9,17,18]

Thus, an improved understanding of CS pharmacogenomic effects from multiple dosing regimens would be required to provide insight into the underlying molecular mechanisms of action. In this direction, our earlier work had focused on assessing transcriptional dynamics to (1) identify transcriptional modules of characteristic mRNA dynamic features across multiple dosing regimens of CSs and (2) elaborate on their common regulatory controls.[9,17,18]

However, pharmacological time-series obtained from different (transcriptomic or other) platforms and time-scales, including multiple dosing regimens,[5,19] complicate the analysis. Several approaches have been proposed and are generally classified into two main categories: (1) integrate profiles from different studies into one dataset so that available analysis tools can be directly applied to the concatenated dataset or (2) analyze and interpret each dataset separately and subsequently compare the analysis (meta-analysis).[20–27] Since combining data across different platforms remains a serious challenge, meta-analysis approaches are gaining popularity[28,29] given the underlying hypothesis is that even though raw data may not be comparable, the results of the individual analyses are.

As an alternative to the meta-analysis approach, we recently proposed the mapping of transcriptomic data onto signaling and metabolic pathways which are scored based on the emerging activity of the pathway, as manifested via the obtained transcriptional data.[30–33] The pathway scoring expresses the overall, intrinsic dynamic of the pathway and its score does not rely on measuring a consistent set of transcriptional profiles across the various conditions—provided the score can be robustly determined (see "Methods" section).

In this study, we extend and expand our earlier framework and present an integrated approach for decomposing transcriptomic-based pathway activities enabling the characterization of (1) the emerging transcriptional dynamics in response to MPL and (2) the dosing-dependent implications induced due to differences in drug exposure (acute vs chronic). We analyzed acute and chronic MPL dosing in male adrenalectomized (ADX) rats and characterized the dosing-dependent differences in the dynamic response of MPL-responsive signaling and metabolic pathways, including the following: lipid metabolism,[34,35] amino acid metabolism,[36,37] carbohydrate metabolism,[38,39] metabolism of cofactors and vitamins,[40] regulation of essential organelles,[41-43] and xenobiotic metabolism pathway groups.[44] To further elucidate, and consistently compare dosing-induced changes in the dynamics of pathway activities, we propose a novel model-based assessment of pathway dynamics, extending the principles of pharmacokinetics/pharmacodynamics (PKPD) to describe pathway activities. The model-based approach enabled us to hypothesize on the likely emergence (or disappearance) of multiple dosing-dependent regulatory interactions, pointing to likely mechanistic implications of dosing of MPL upon transcriptional regulation.

Methods

Animal model and experimental data

Acute dosing. A total of 43 ADX male Wistar rats were treated with a bolus dose of 50 mg/kg MPL intravenously.[19] This dose was established in previous investigations identifying biomarkers for gene-mediated effects of GCs within liver because it produces strong, but not saturating, effects on gene and protein expression within rat liver and for its comparability with large doses in human upon scale-up.[5] Liver is analyzed as a primary site of GC action and contains a relatively high concentration of GC receptors in comparison with other tissues.[46] The animals were sacrificed at 17 timepoints (n = 2-4) from 0 to 72 hours post dosing. Affymetrix GeneChip Rat Genome U34A (Affymetrix, Inc, Santa Clara, CA) was used to array the mRNA expression data collected at these timepoints (microarray contains 8799 probes). The dataset was collected in a previous investigation, submitted to GEO (GSE490), and we have previously presented multiple analyses of the transcription responses.[8–11,33,47]

Chronic dosing. A total of 40 ADX male Wistar rats were administered 0.3 mg/(kg·h) of MPL intravenously for 7 days.[5] As with the acute analysis, liver is analyzed as a primary site of GC action and contains a relatively high concentration of GC receptors in comparison with other tissues.[46] Rats were sacrificed at 11 timepoints (n = 4) from 0 to 168 h.[5] As an additional timepoint at 0 h and as a control, four additional rats were used as a control group at various times throughout 7-day time period.[5] Affymetrix GeneChip Rat Genome 230A (Affymetrix, Inc) was used to analyze the data in the chronic study (microarray contains 15 967 probes). The dataset was collected in a previous investigation, submitted to GEO (GDS972), and we have previously presented multiple analyses of the transcription responses.[9,10,17,18]

Mapping transcriptomic data onto pathways

A pathway can be defined as a network of molecular interactions and reactions designed to link genes in the genome to gene products. Pathways express layered and complementary activities, meaning pathways are groups of genes linked mechanistically that effect a biochemical action. Numerous databases exist describing pathway definition. The Kyoto Encyclopedia of Genes and Genomes (KEGG) pathways is used as the functional grouping instrument. KEGG is one of the most comprehensive and readily used by genomics researchers.[48,49] As of January 2018, this database contains 524 pathways that represent genomic and proteomic information across 5646 organisms, 53 of which are mammals. Of the 524 possible KEGG pathways, 317 are relevant to *Rattus norvegicus*. Pathways unrelated to the liver are irrelevant to this study of MPL influence within the liver. For this reason, pathways unrelated to the liver (eg cardiac muscle contraction, complement and coagulation cascades, and platelet activation), describing neurological diseases (eg non-alcoholic fatty liver disease, Alzheimer disease, Parkinson disease, and Huntington disease), irrelevant to the liver (olfactory transduction), or redundant for all other metabolic pathways (KEGG's pathway titled Metabolic pathways rno:01100 is the set of all other metabolism-related pathways) are removed from the pathway set. The final list used for this investigation totals 209 pathways relevant to the liver.

To begin characterizing the liver response to MPL, the microarray data are contextualized by identifying which of the 209 liver-relevant pathways are populated by it. Fractional coverage (f_c) is calculated for each pathway, a fraction that communicates the number of unique genes (rno) identified within the microarray data relative to the number of genes within the KEGG pathway (equation 1). The metric quantifies the extent to which a pathway is represented in the dataset and is reported in the genome-wide transcriptomic studies. This step requires a series of probe name conversions facilitated by additional databases: DAVID[50,51] and UniProt.[52] Genes from rat pathways in KEGG are recognized by the identifier, *rno*. UniProt is used to convert from rno to UniProt accession numbers. Only genes reported as reviewed in UniProt were retained. These are then converted to Affymetrix probe identifiers within the DAVID database. Affymetrix probes are redundant meaning multiple Affymetrix identifiers will refer to a single protein accession ID. However, one rno ID refers to a single unique protein accession number:

$$f_c = \frac{rno \text{ in Dataset}}{rno \text{ in KEGG Pathway}}. \tag{1}$$

To assess the confidence in the fractional coverage, an associated p-value (f_c p-value) is calculated. Confidence in f_c is important for two reasons: (1) to quantify the extent to which the fractional coverage of a pathway based on the specific experiment could have been obtained by a random collection of genes and (2) more importantly, since different experiments may not be quantifying the same subsets of pathway-specific genes, we need to establish significant coverage based on different subsets. The significance of the f_c is determined using the one-tail Fisher exact test such that the total rat genome is the set of unique rat genes in all of KEGG's rat-relevant pathways.

A pathway is considered significant if its f_c p-value meets a user-defined threshold. For this investigation, a p-value threshold of 10^{-3} is used to identify the pathways considered significantly represented. Pathway activity analysis further refines this list of significant pathways by determining which pathways are significantly active.

A pathway may yield a high f_c value but contain a small population of actual genes. The selection of the list of significant pathways that make up the pathway solution set is presented in the "Results" section. In the process of determining this list of significant pathways, the actual gene population for each pathway is necessary to consider. In addition, determining whether a set of pathways is significant involves consideration of the average actual gene count for the set. An average *rno* (rno_{avg}) is calculated for a pathway solution set. The significance of this statistic is reported as a p-value (rno_{avg} p-value) calculated using a bootstrapping technique (equation 2). Given a pathway set containing P pathways, N random pathway sets of length P are selected and rno'_{avg} is calculated for each. The distribution of rno'_{avg} is compared against the rno_{avg} from the original set of P pathways yielding n pathways with rno'_{avg} greater than rno_{avg} :

$$rno_{avg}\ p\text{-}value = \frac{n_{(rno'_{avg} > rno_{avg})}}{N}. \tag{2}$$

Pathway activity analysis

Methylprednisolone administration is the impetus for genomic activity, directly and indirectly, within the datasets considered in this investigation. Pathways determined to have significant fractional coverage are analyzed with pathway activity analysis (Figure 1). This component of the analysis determines whether a pathway is active without eliminating individual genes; no gene expression profiles are eliminated using conventional differential expression analysis and user-defined threshold cutoff.[53] Instead, singular value decomposition (SVD) is used to identify global and subtle expression trends within the pathway gene sets.

Pathway analysis assumes that pathways exhibit layered behaviors of subgroups of genes. Singular value decomposition is used as a dimension reduction technique, reducing temporal gene expression datasets into sets of singular vectors and singular values that communicate global trends and relative trend dominance.[30-33] (As a preprocessing step before application of SVD pathway activity analysis, gene expression profiles are z-scored.) This technique is previously applied within investigations assessing for subtle circadian rhythmicity in genes that otherwise are not recognized as differentially expressed[33] and for identifying the effects of dibutyl phthalate in male reproductive organ development.[30-32] Within this investigation, complex tissue-specific behavior is revealed by the SVD decomposition of pathway gene sets.

Application of SVD to a pathway gene set yields two translational matrices (U and V) and an singular value matrix (S) (Figure 2). The subtle global trends within the pathways are the activities of metagenes, an abstract object that captures dominant characteristics common to many gene expression profiles within the dataset. The "expression" or activity of a metagene over time is defined as the pathway activity level (PAL) profile. Pathway activity level profiles are found within the row vectors of the transpose of the translational matrix V (ie PAL profiles are the row vectors of V^T) denoted in equation 3.

The dominance of each metagene's activity is preserved in the order in which the PAL profiles appear descending in V^T as well as in the diagonal of the singular value matrix (S); the most dominant metagene appears first. To quantify this

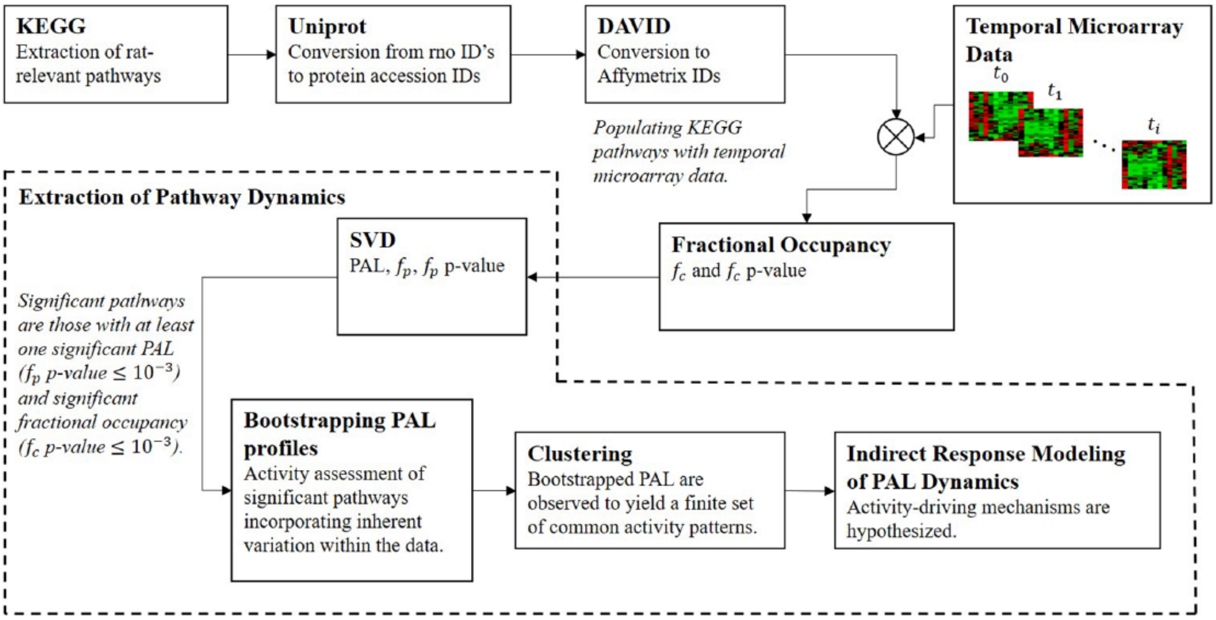

Figure 1. Method of significant pathway assessment and comparison.

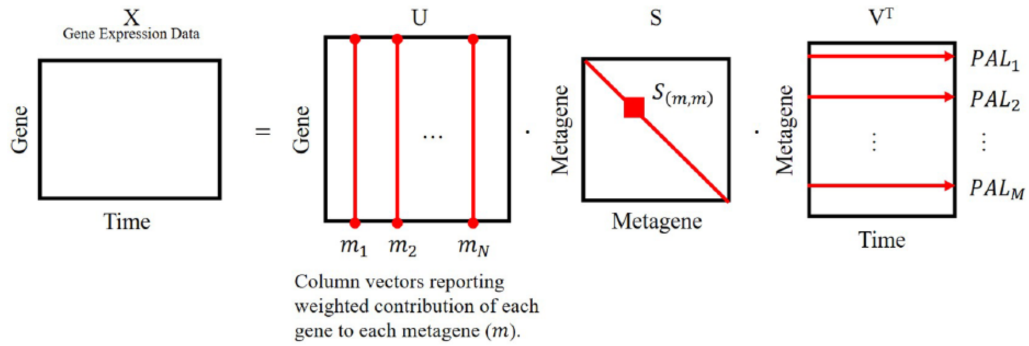

Figure 2. Singular value decomposition (SVD) of a pathway gene set. A pathway matrix (X) designed such that each row is a unique gene and columns are samples at each timepoint from 0 to 72 hours. SVD yields (1) matrices U (translational matrix) in which the rows are individual genes and columns indicate a gene's match to a metagene (G genes make up a gene set and M metagenes results from SVD where the number of metagenes is equal to the number of sample times.); (2) matrix S, a diagonal singular value matrix reporting the dominance of each metagene; and (3) matrix V, the transform denoted V^T, an additional translational matrix in which the rows of V^T indicate each metagene and the columns indicate time. Pathway activity level profiles are taken as metagene expression over time—the rows of V^T.

dominance, the singular values within the diagonal of matrix S are normalized by the sum of the diagonal (equation 4) to yield the fraction of pathway activity of a PAL defined as the f_p statistic.[33] Each PAL describes a pathway activity profile and corresponds to a unique f_p value which reports the percent of total pathway activity represented by that PAL.

The number of PAL profiles reported by V^T is equal to the number of samples (timepoints). However, not all patterns are significant. To determine PAL significance, a bootstrapping calculation is used to generate a p-value associated with f_p statistic. The original gene set is bootstrapped ($N = 1000$). Bootstrapped gene sets are constructed by scrambling the pathway gene set N times.[54] Each bootstrapped pathway gene set is decomposed with SVD, yielding N sets of PAL' profiles and associated f_p' values for each PAL' profile. For each PAL, the distribution of f_p' values which results from the bootstrapped pathway gene sets is compared with the original f_p values. The number of f_p' greater than an f_p is divided by N to determine whether each f_p (and by association the PAL) is likely to emerge from a randomized gene set (equation 5).

This investigation seeks to characterize the consequences of MPL within the liver from a pathway perspective. However, the correlation of each metagene to each gene is important to our understanding of the consequences of MPL and is identified within the translational matrix U. Rows of U correspond to genes and columns to metagenes. The correlation of each gene (g) to each metagene (m) is defined as $W_{g,m}$ (equation 6). The correlation of each gene to each metagene ($W_{g,m}$) is the correlation of each gene expression profile to each PAL profile.

Thus, global trends (PAL) in a gene set each have an associated fraction of the pathway activity (f_p) that they capture. Multiple significant PAL may emerge for each gene set, and each gene's correlation to each PAL is given by its weight. Pathway activity levels are also symmetric, thus two PAL profiles, of opposite sign but equal magnitude, indicate the same expression activity events.

The list of pathways with significant fractional coverage (f_c p-value $\leqslant 10^{-3}$) is further reduced to the list of pathways that also yield significant pathway activity. Pathways capable of generating at least one significant PAL profile are considered significant and a PAL profile is significant if its corresponding f_P p-value $\leqslant 10^{-3}$:

$$PAL_m = V^T(m,\bar{t}), \tag{3}$$

$$f_P = \frac{S(m,m)^2}{\sum_{m=1}^{M} S(m,m)^2}, \tag{4}$$

$$f_P \; p\text{-}value = \frac{n(f_P' > f_P)}{N}, \tag{5}$$

$$W_{g,m} = U(g,m). \tag{6}$$

Prediction of pathway activity with bootstrapping

Variability in the expression data indicates that the influence of MPL within the liver is not uniform with each administration. To account for the variability, a bootstrapping approach is used to generate pathway gene sets likely to exist given additional MPL dosing studies which are then assessed for pathway activity. In this component of the investigation, the range of activity capable of emerging from the system is investigated.

Bootstrapped gene sets are constructed from bootstrapped gene expression profiles, where each profile is projected within a normal distribution about the gene's average expression. In short, each gene expression profile is bootstrapped within a normal distribution about the gene expression profile's mean. The bootstrapped genes are assembled into appropriate pathway gene sets, ultimately yielding N bootstrapped pathway gene sets for each pathway ($N = 1000$ bootstrapped gene sets per pathway). Each of these bootstrapped pathway gene sets is decomposed with SVD. Significant PAL profiles identified from these bootstrapped genes and their corresponding f_P and f_P p-value statistics are retained for each significant pathway. All PAL profiles extracted from these bootstrapped gene sets are assumed likely system behavior that would emerge if the rat experiments were repeated.

For each pathway, the significant bootstrapped PALs are clustered such that common activity patterns group together. The MATLAB® function *evalclusters.m* is applied to assess optimal cluster number using the gap statistic and applying k-means clustering.[55] Thus, a finite set of PAL centroids are identified, indicating that a finite list of activity patterns are induced by MPL to emerge from each pathway.

Evaluating pathway dynamics

The pathway activity analysis decomposes a pathway's intrinsic dynamics into its leading, independent constitutive elements. To compare activities based on non-overlapping gene sets, across dosing regimens of different time horizons, we introduce a novel model-based approach, where the dynamics of each dominant PAL is approximated using PKPD-driven models exploring alternative hypotheses for the mechanisms of regulation of a pathway.

Pharmacokinetics. The PK of MPL in both regimens was shown to be appropriately described by a two-compartment model (Figure 3; equations 7 and 8).[18,56] A_p and A_t denote drug in the plasma and tissue compartments, respectively. Term k_0 is the zero-order rate constant for drug input into the plasma, CL indicates clearance, V_p indicates plasma volume of distribution, and k_{12} and k_{21} are the intercompartmental distribution rate constants. In the case of acute MPL administration, $k_0 = 0$ indicates a bolus injection. Parameter values are adopted from the study of Ramakrishnan et al and presented in Table 1[18,56]:

$$\frac{dA_p}{dt} = k_0 + k_{21} \cdot A_t - \left(k_{12} + \frac{CL}{V_p}\right) \cdot A_p, \tag{7}$$

$$\frac{dA_t}{dt} = k_{12} \cdot A_p - k_{21} \cdot A_t. \tag{8}$$

Receptor dynamics. Methylprednisolone action is receptor mediated (Figure 3; equations 9-12).[18,56,57] Parameter values are adopted from the work of Hazra et al[18] and presented in Table 2. Here, R_m indicates the mRNA of the free cytosolic receptor, R indicates the free cytosolic receptor, DR indicates the cytosolic drug-receptor complex, and DRN indicates the drug-receptor complex in the nucleus.[56] The concentration at which the synthesis rate of receptor mRNA drops to 50% of its baseline value is indicated by IC_{50Rm} parameter. Parameter k_{on} indicates the second-order rate constant for drug-receptor binding. Parameters k_T and k_{re} are the first-order rates of receptor translocation between the nucleus and the cytosol (k_{re} to the nucleus; k_{re}: recycling back to the nucleus).[56] The fraction of receptor recycled is indicated by parameter R_f. C_{MPL} corresponds to the concentration of free receptor in the cytosol and is determined by the equation $C_{MPL} = 0.43(A_p / V_p)$ where 0.43 is the fraction of unbound MPL within the cytosol[18,56]:

$$\frac{dRm}{dt} = k_{sRm} \cdot \left(1 - \frac{DRN}{IC_{50Rm} + DRN}\right) - k_{dRm} \cdot Rm, \tag{9}$$

$$\frac{dR}{dt} = k_{sR} \cdot Rm + R_f \cdot k_{re} \cdot DRN - k_{on} \cdot C_{MPL} \cdot R - k_{dR} \cdot R, \tag{10}$$

$$\frac{dDR}{dt} = k_{on} \cdot C_{MPL} \cdot R - k_T \cdot DR, \tag{11}$$

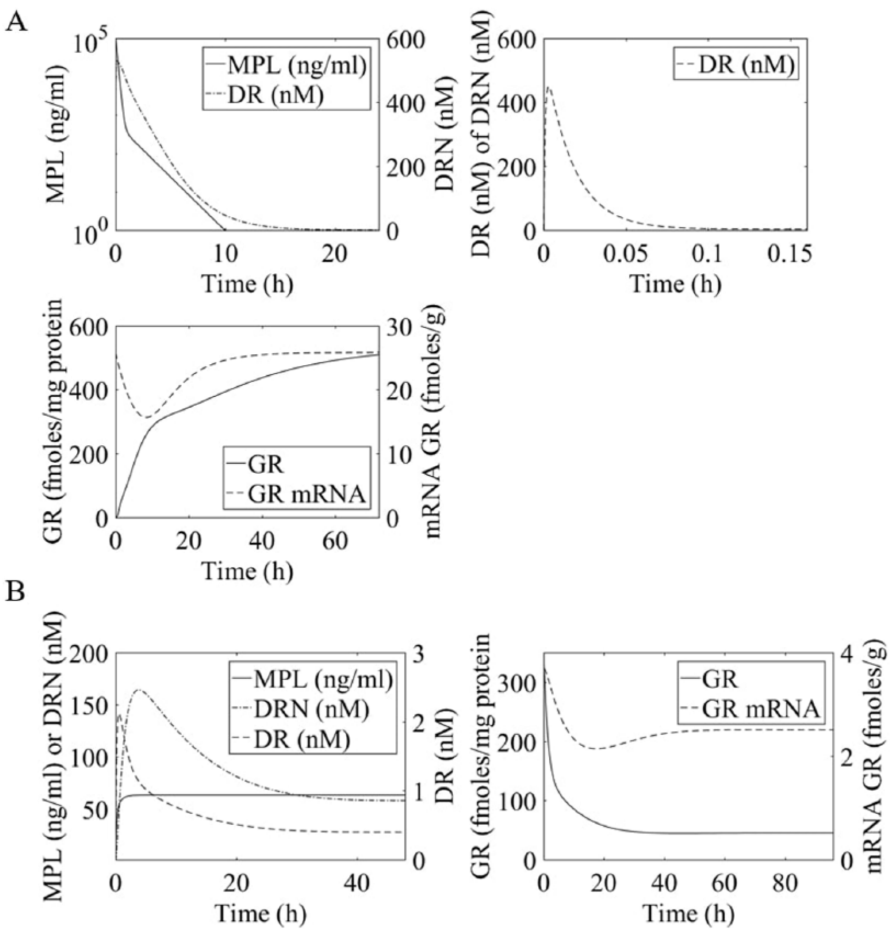

Figure 3. Time profiles of MPL pharmacokinetics and receptor dynamics for (A) acute 50 mg/mL bolus MPL dose and (B) chronic infusion of 0.3 mg/(kg·h) MPL. Methylprednisolone influence over transcription within the liver is dosing dependent and receptor mediated.[18,19,56–59]

Table 1. Pharmacokinetic parameters of acute and chronic MPL administration.[56]

PARAMETER	DEFINITION	ACUTE	CHRONIC
$k_0 \left(\frac{1}{h}\right)$	Rate of drug concentration into central plasma compartment	0	220
CL $\left(\frac{l}{h \cdot kg}\right)$	Clearance	3.48	5.61
$V_p \left(\frac{l}{kg}\right)$	Central volume of drug distribution	0.73	0.82
$k_{12} \left(\frac{1}{h}\right)$	Drug distribution rate constant	0.98	0.32
$k_{21} \left(\frac{1}{h}\right)$	Drug distribution rate constant	1.78	0.68

$$\frac{dDRN}{dt} = k_T \cdot DR - k_{re} \cdot DRN. \tag{12}$$

Pathway pharmacodynamics. Once a pathway's activity has been decomposed to its constitutive intrinsic components, we characterize its dynamics in a model-based manner by assuming that each PAL is approximated by an appropriate dynamic model. Comparisons across dosing regimens are then performed in the space of models as opposed to the space of transcriptional data. We hypothesized (based on the results to be discussed shortly) that the dynamic decomposition of the pathway activity indicates components whose transcription is regulated by an MPL-receptor complex (DRN) binding to a GRE element in the nucleus and regulated by transcription mediated by MPL binding to an intermediate biosignal (BS)—interestingly, this was dosing dependent. In this direction, we extend the concepts described in the studies of Yao et al[17] and Hazra et al.[18] The simpler mode of pathway regulation assumes a saturable induction of the pathway activity (Figure 4A; equation 13) where k_s indicates the activation rate of pathway activity, IC_{50PAL} indicates the concentration of DRN responsible for 50% inhibition of the pathway activity activation rate, and k_d indicates the deactivation rate of pathway activity. This mode is expected to reflect "monophasic" dynamics with a transient (acute dosing) or persistent (chronic dosing) deviation of a pathway's activity following i.v. MPL administration. In addition, the emergence of regulation mediated through an MPL-regulated BS is likely to exhibit a "biphasic" response (Figure 4B; equations

Table 2. Parameters for receptor-mediated effects of acute and chronic MPL administration.[18]

PARAMETER	DEFINITION	ACUTE	CHRONIC
$k_{sRm}\left(\frac{fmol}{g\cdot h}\right)$	Receptor mRNA synthesis rate constant	3.15	0.45
$k_{dRm}\left(\frac{1}{h}\right)$	Receptor mRNA degradation rate constant	0.122	
$IC_{50Rm}\left(\frac{nmol}{L\cdot mg_{protein}}\right)$	DRN required for 50% inhibition of the synthesis rate of *Rm*	123.7	
$k_{sR}\left(\frac{nmol}{L\cdot mg_{protein}\cdot fmol_{Rm}\cdot g\cdot h}\right)$	Receptor synthesis rate	0.84	3.63
$k_{re}\left(\frac{1}{h}\right)$	Loss rate for drug receptor in the nucleus	0.402	
$k_{on}\left(\frac{l}{nmol\cdot h}\right)$	Association rate for receptor-drug binding	0.019	
$k_{dR}\left(\frac{1}{h}\right)$	Receptor loss/degradation rate	0.0403	
$k_{T}\left(\frac{1}{h}\right)$	Translocation of receptor into the nucleus	58.1	
R_f	Receptor recycling factor from nucleus to cytosol	0.69	

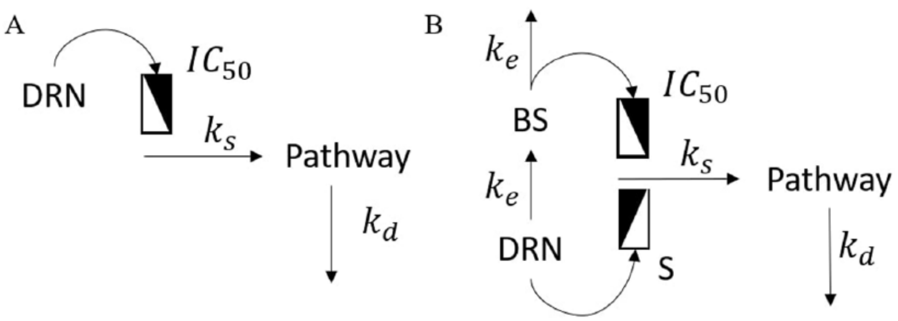

Figure 4. Regulatory mechanism schematics for the (A) monophasic activity model and (B) biphasic activity model adapted from the study of Hazra et al.[18] (A) Methylprednisolone regulates transcription via binding to glucocorticoid receptors within the cytosol, transporting into the nucleus, and binding to a GRE element thus initiating targeted transcription, as captured by the monophasic model. (B) The biphasic model describes this GRE-binding activity in combination with an additional mechanism of MPL regulation, that of binding to an intermediate biosignal (BS) which influences targeted transcription rate.[18,19,56–59]

14 and 15), describing the dynamics of an intermediate BS whose synthesis is directly related to DRN by k_e, S is the stimulation constant for pathway activity due to DRN, IC_{50PAL} indicates the BS responsible for 50% inhibition of pathway activity activation rate, and γ indicates the factor of amplification of the influence of BS on the activation of pathway activity. These model equations are adapted from the transcription regulatory models of Hazra et al,[18] where alternative models were also discussed, and could be easily accommodated. However, our analysis indicated that these simpler forms captured the essence of the pathway dynamics.

Monophasic activity.

$$\frac{dPAL}{dt} = k_s\left(1 \pm \frac{DRN}{IC_{50PAL} - DRN}\right) - k_d \cdot PAL. \qquad (13)$$

Biphasic activity.

$$\frac{dBS}{dt} = k_e\left(DRN - BS\right). \qquad (14)$$

$$\frac{dPAL}{dt} = k_s\left(1 \pm S\cdot DRN\right)\left(1 \mp \frac{BS^{\gamma}}{IC_{50PAL}^{\gamma} - BS^{\gamma}}\right) - k_d \cdot PAL. \qquad (15)$$

Parameter estimation was performed using MATLAB's optimization toolkit in a series of optimization stages. In all stages, we sought to minimize the residual sum of squares between the model prediction and the cluster centroid profile. In the first stage, it is assumed that the system is nonlinear and neither continuous nor differentiable for the entire parameter solution space. Therefore, as a rapid preliminary global search for a minimum, a stochastic direct method (simulated annealing) with bound constraints is employed. The result of this global search technique is taken as the initial parameter values for the second optimization stage using a direct pattern search method. In the final stage, a gradient-based method is used to probe this more limited space as the final optimization step. This stage uses the sequential quadratic programming as implemented through MATLAB's *fmincon*. The model which results from this optimization process is visually inspected.

Results

Fractional coverage analysis of the 209 rat/liver-relevant KEGG pathways yields 56 and 57 pathways as significant, for acute and chronic dosing, respectively. These are decomposed to their constitutive activities with the SVD approach described earlier. Each pathway yields multiple PAL profiles of varying significance. A fraction of total pathway activity (f_p) is identified for each PAL and only significant f_p indicate significant PAL. To assess the significance of the coverage, we also calculate the confidence for each f_p value, defined as the f_p *p*-value and described in the "Pathway activity analysis" section.

For consistency, the *p*-value threshold of 10^{-3} is used for selecting both the over-represented pathways and the significant f_p values. A significant f_p corresponds to a PAL profile. A pathway is robustly active if its activity is described by at least one significant PAL. This analysis yields 26 significant pathways in the acute and 27 in the chronic datasets. Interestingly, we identify that the subset of 24 active pathways are shared across both dosing regimens, albeit the patterns of activity observed within the PAL are different—as will be discussed in greater detail in the "Discussion" section.

Table 3 reports the details of the 24 pathways active in both the acute and the chronic data. For each pathway, fractional coverage ((f_c) is reported in the acute and chronic datasets. Also reported in this table are total f_p values for pathway datasets of different significance thresholds. In the original gene set of each pathway, significant PALs are identified, each corresponding to an independent f_p value. The total of these significant f_p values indicates the fraction of pathway activity that is significant. This total fraction of pathway activity is what is reported as the total f_p value within this table.

Bootstrapping each pathway dataset allows us to identify, in silico, likely activity patterns from synthetic replications (bootstrapped) of the animal studies which yielded the transcriptomic datasets. A total of 1000 bootstrapped datasets were generated for each pathway and significant pathway activities (PAL profiles) were identified, as described in the "Methods" section. We repeatedly identified significant pathway activities within the bootstrapped pathway gene sets and identified common patterns of activity despite the variability of the original data.

Pathways decomposed each into multiple PALs, indicating a likely codominance of activity patterns within the pathway and complex regulation of the pathways' components. To consistently characterize the dynamics of each individual PAL for a given pathway, we hypothesize likely modes of regulation. Namely, we hypothesize a PAL component is either directly or indirectly regulated by MPL and possibly an intermediate BS. The dynamics of each PAL are fitted using either the monophasic or biphasic regulatory models, as described in the "Evaluating pathway dynamics" section. This step is critical as it allows us to compare PAL dynamics within, and across, dosing regimens in a model-based, data-independent manner.

Detailed analysis of the common pathways revealed very interesting trends. Using the acute response as the basis, we identify two class groupings within the set of 24 significant pathways: Class 1 (acute monophasic or acute biphasic response): pathways exhibiting either monophasic or biphasic regulation only; Class 2 (acute monophasic and acute biphasic, also known as complex acute): pathways exhibiting both monophasic and biphasic activities, that is, individual pathways that yield multiple PALs, some of which are acute monophasic and some of which are acute biphasic. Within these primary categories based on acute data, we further investigated the type of regulation each of the pathways under chronic dosing. Table 4 presents each pathway and its categorization by class and response type.

Class 1: exclusively monophasic or biphasic acute response

Overall, 12 pathways are identified with strictly acute monophasic responses and one pathway exhibits strictly acute biphasic response. The acute monophasic response pathways are classified by pathway families including amino acid metabolism (beta-alanine metabolism; glutathione metabolism; tryptophan metabolism; and valine, leucine, and isoleucine degradation),[36,37] carbohydrate metabolism (propanoate metabolism),[38,39] essential organelle regulation (peroxisome and proteasome),[41–43] lipid metabolism (fatty acid degradation, fatty acid metabolism, peroxisome proliferator-activated receptor [PPAR] signaling pathway, and steroid hormone biosynthesis),[34,35] and metabolism of cofactors and vitamins (retinol metabolism).[40] Most of the monophasic responses in this set yield an early monophasic response, which consists of a single peak of activity corresponding to the direct effect of DRN between 2 and 5 hours (also referenced as DRN effect peak) and subsequent return to initial baseline between 18 and 30 hours. The proteasome pathway exists as an outlier by

Table 3. Significant pathways common to acute and chronic dosing data. These pathways exhibit significant fractional coverage (f_c p-value $\leqslant 10^{-3}$) and significant pathway activity (f_p p-value $\leqslant 10^{-3}$) in both the acute and the chronic datasets.

PATHWAY	RNO ID	ACUTE					CHRONIC				
		UNIQUE GENES IN PATHWAY FROM DATASET (RNO)	FRACTIONAL PATHWAY COVERAGE (f_c), %	TOTAL SIGNIFICANT FRACTION OF PATHWAY ACTIVITY (TOTAL f_P)			UNIQUE GENES IN PATHWAY FROM DATASET (RNO)	FRACTIONAL PATHWAY COVERAGE (f_c), %	TOTAL SIGNIFICANT FRACTION OF PATHWAY ACTIVITY (TOTAL f_P)		
				PATHWAYS P-VALUE ⩽ .1, %	PATHWAYS P-VALUE ⩽ .01, %	PATHWAYS P-VALUE ⩽ .001, %			PATHWAYS P-VALUE ⩽ .1, %	PATHWAYS P-VALUE ⩽ .01, %	PATHWAYS P-VALUE ⩽ .001, %
Amino acid metabolism											
Arginine biosynthesis	rno:00220	11	55	76	76	76	11	55	54	54	54
Biosynthesis of amino acids	rno:01230	27	32	73	73	73	33	39	76	76	76
Cysteine and methionine metabolism	rno:00270	17	36	70	70	70	19	40	65	65	65
Valine, leucine, and isoleucine degradation	rno:00280	25	45	58	58	58	29	52	51	51	51
Beta-alanine metabolism	rno:00410	12	36	66	66	66	16	48	75	52	52
Tryptophan metabolism	rno:00380	16	34	61	61	61	25	53	65	65	65
Glutathione metabolism	rno:00480	17	26	65	65	65	22	34	66	66	66
Carbohydrate metabolism											
Citrate cycle (TCA cycle)	rno:00020	13	39	71	71	71	19	58	82	82	61
Pyruvate metabolism	rno:00620	13	33	68	68	68	15	38	68	68	42
Carbon metabolism	rno:01200	39	31	68	68	68	57	45	84	72	72
Oxidative phosphorylation	rno:00190	37	26	74	74	74	49	34	63	63	63
Glycolysis/gluconeogenesis	rno:00010	18	25	72	72	72	25	35	64	64	64
Propanoate metabolism	rno:00640	13	41	57	57	57	15	47	45	45	45
Glyoxylate and dicarboxylate metabolism	rno:00630	10	36	49	49	49	14	50	51	51	27
Essential organelles											
Proteasome	rno:03050	18	38	80	64	64	20	42	58	58	58
Peroxisome	rno:04146	26	30	59	59	59	33	38	63	63	63
Ribosome	rno:03010	59	33	81	81	81	82	46	78	78	78

(Continued)

Table 3. (Continued)

PATHWAY	RNO ID	ACUTE					CHRONIC				
		UNIQUE GENES IN PATHWAY FROM DATASET (RNO)	FRACTIONAL PATHWAY COVERAGE (f_c), %	TOTAL SIGNIFICANT FRACTION OF PATHWAY ACTIVITY (TOTAL f_P)			UNIQUE GENES IN PATHWAY FROM DATASET (RNO)	FRACTIONAL PATHWAY COVERAGE (f_c), %	TOTAL SIGNIFICANT FRACTION OF PATHWAY ACTIVITY (TOTAL f_P)		
				PATHWAYS *P*-VALUE ⩽ .1, %	PATHWAYS *P*-VALUE ⩽ .01, %	PATHWAYS *P*-VALUE ⩽ .001, %			PATHWAYS *P*-VALUE ⩽ .1, %	PATHWAYS *P*-VALUE ⩽ .01, %	PATHWAYS *P*-VALUE ⩽ .001, %
Protein processing in endoplasmic reticulum	rno:04141	32	19	65	65	65	54	33	65	65	65
Lipid metabolism											
Fatty acid degradation	rno:00071	28	60	56	56	56	27	57	63	63	43
Fatty acid metabolism	rno:01212	26	48	71	56	56	25	46	65	46	46
Steroid hormone biosynthesis	rno:00140	27	33	69	55	55	26	31	64	64	43
PPAR signaling pathway	rno:03320	26	32	52	52	52	25	30	66	66	66
Xenobiotic metabolism											
Metabolism of xenobiotics by cytochrome P450	rno:00980	22	30	76	76	61	23	32	71	71	71
Metabolism of cofactors and vitamins											
Retinol metabolism	rno:00830	24	28	55	55	55	25	29	66	66	66

Abbreviations: PPAR, peroxisome proliferator-activated receptor; TCA, tricarboxylic acid cycle.

Table 4. Responses of significant (f_p p-value and f_c p-value $\leqslant 10^{-3}$) pathways to acute and chronic MPL administration.

PATHWAY	PATHWAY CATEGORY	ACUTE MPL RESPONSE	CHRONIC MPL RESPONSE	CLASS
Glyoxylate and dicarboxylate metabolism	Carbohydrate metabolism	Biphasic	Monophasic	1
Tryptophan metabolism	Amino acid metabolism	Monophasic	Biphasic	1
Valine, leucine, and isoleucine degradation	Amino acid metabolism	Monophasic	Monophasic/biphasic	1
Propanoate metabolism	Carbohydrate metabolism	Monophasic	Biphasic	1
Peroxisome	Essential organelles	Monophasic	Monophasic/biphasic	1
Fatty acid degradation	Lipid metabolism	Monophasic	Monophasic/biphasic	1
Steroid hormone biosynthesis	Lipid metabolism	Monophasic	Monophasic/biphasic	1
Fatty acid metabolism	Lipid metabolism	Monophasic	Monophasic/biphasic	1
PPAR signaling pathway	Lipid metabolism	Monophasic	Monophasic/biphasic	1
Beta-alanine metabolism	Amino acid metabolism	Monophasic	Monophasic	1
Glutathione metabolism	Amino acid metabolism	Monophasic	Monophasic	1
Proteasome	Essential organelles	Monophasic	Monophasic	1
Retinol metabolism	Metabolism of cofactors and vitamins	Monophasic	Monophasic	1
Citrate cycle (TCA cycle)	Carbohydrate metabolism	Monophasic/biphasic	Biphasic	2
Pyruvate metabolism	Carbohydrate metabolism	Monophasic/biphasic	Biphasic	2
Ribosome	Essential organelles	Monophasic/biphasic	Biphasic	2
Metabolism of xenobiotics by cytochrome P450	Xenobiotic metabolism	Monophasic/biphasic	Biphasic	2
Arginine biosynthesis	Amino acid metabolism	Monophasic/biphasic	Monophasic	2
Oxidative phosphorylation	Carbohydrate metabolism	Monophasic/biphasic	Monophasic	2
Biosynthesis of amino acids	Amino acid metabolism	Monophasic/biphasic	Monophasic/biphasic	2
Cysteine and methionine metabolism	Amino acid metabolism	Monophasic/biphasic	Monophasic/biphasic	2
Glycolysis/gluconeogenesis	Carbohydrate metabolism	Monophasic/biphasic	Monophasic/biphasic	2
Carbon metabolism	Carbohydrate metabolism	Monophasic/biphasic	Monophasic/biphasic	2
Protein processing in endoplasmic reticulum	Essential organelles	Monophasic/biphasic	Monophasic/biphasic	2

Abbreviations: MPL, methylprednisolone; PPAR, peroxisome proliferator-activated receptor; TCA, tricarboxylic acid cycle.

exhibiting a late monophasic response consisting of a delayed DRN event peak between 7 and 15 hours and a return to baseline between 32 and 65 hours, defining the late biphasic response category. Only the glyoxylate and dicarboxylate metabolism pathway, within the carbohydrate metabolism family, exhibits a biphasic response to acute MPL administration, discussed further below.

Although many pathways exhibit monophasic behavior in response to either acute or chronic dosing, the glutathione metabolism, retinol metabolism, proteasome, and beta-alanine metabolism pathways exhibit exclusively monophasic behavior in response to both acute and chronic dosing. The acute response for each of these pathways reports a DRN event peak between 3 and 4 hours followed by a return to baseline between 20 and 25 hours. In the glutathione metabolism pathway, chronic MPL administration yields a steep and continuous incline and does not settle to a new steady-state value within the 168 hours of the experiment. The beta-alanine pathway yields strictly one pattern of behavior in response to chronic MPL, a steep incline until 25 hours followed by a settling to a new steady state by 120 hours. The retinol metabolism pathway returns multiple chronic behavior responses: a steep continuous incline with no peak and no settling to a new baseline within the experiment time; steep incline until 25 hours followed by settling at a new steady state by 120 hours; and peak DRN activity event at 22 hours followed by a settling at a new steady state by 55 hours. The proteasome pathway exhibits a slightly later acute DRN event peak at 9 hours and returns to baseline by 50 hours. The proteasome pathway is singular in that its response to chronic MPL administration yields DRN event peaks between 12 and 16 hours followed by settling to a new steady state by 50 hours.

Two pathways, propanoate metabolism and tryptophan metabolism, exhibit a DRN event peak at 3 hours and a return to baseline by 20 to 25 hours in response to acute MPL administration. In response to chronic MPL administration, these pathways exhibit strictly biphasic behavior. Propanoate metabolism yields a DRN peak between 11 and 17 hours, and a peak activity event due to an intermediate BS between 40 and 44 hours. This pathway does not settle to a new steady state within the 168-hour timeframe of the experiment, but the approach to an asymptote is implied. Tryptophan metabolism reports similar behavior, yielding a DRN event peak at 16 hours, an intermediate BS peak between 44 and 54 hours, and approaches an asymptote either by 150 hours or is implied to approach steady state outside of the 168-hexperimental period.

The remaining six pathways (fatty acid degradation; fatty acid metabolism; peroxisome; PPAR signaling pathway; steroid hormone biosynthesis; and valine, leucine, and isoleucine degradation) exhibit the acute response (DRN peak between 3 and 4 hours and return to baseline by 20-25 hours), as well as both monophasic and biphasic responses to chronic MPL administration. Within the lipid metabolism pathways, fatty acid degradation yields monophasic responses with DRN event peaks between 22 and 24 hours followed by a rapid steady-state achievement at 25 hours or a delayed steady-state achievement by 55 hours. This pathway's biphasic responses yield peak DRN events at 15 to 16 hours, intermediate BS events at 40 to 41 hours, and settle to a new activity baseline by 155 hours or after 168 hours. Fatty acid metabolism returns monophasic reporting steep inclines in activity until 25 hours and a similar settling to a new steady state achieved rapidly by 35 hours or with delay by 90 hours. Fatty acid metabolism pathway's chronic biphasic response reports DRN event peaks at 14 hours, intermediate BS event peaks at 33 to 36 hours, and new steady-state achievement either rapidly by 115 hours or is implied to approach a new steady state after the 168 hours.

Relatedly within the lipid metabolism family, PPAR signaling pathway and steroid hormone biosynthesis pathway exhibit steep inclines until 30 to 35 hours in their monophasic response to chronic MPL administration. This is followed by achievement of a new steady state of activity by 90 to 110 hours. The chronic biphasic response within the PPAR signaling pathway describes DRN peaks from 15 to 16 hours, intermediate BS peaks from 34 to 38 hours, and new steady-state achievement by 125 or 130 hours or are implied to achieve steady state after 168 hours by their approach to an activity asymptote. The steroid hormone biosynthesis pathway exhibits one biphasic response that reports a DRN event peak at 1 hour, an intermediate BS event peak at 30 hours, and does not appear to achieve steady state within 168 hours.

Glyoxylate and dicarboxylate metabolism pathway exhibits strictly early biphasic response to acute MPL administration and represents the pathway family carbohydrate metabolism. Early biphasic response is defined by pathways exhibiting DRN effect peaks between 1 and 5 hours, an intermediate BS peak between 12 and 20 hours, and return to baseline between 38 and 65 hours. In response to acute MPL administration, this pathway exhibits DRN event peaks between 4 and 5 hours, intermediate BS event peaks between 16 and 19 hours, and return to baseline between 57 and 65 hours. In response to chronic MPL administration, glyoxylate and dicarboxylate metabolism pathway yields a monophasic response reporting a steep incline until 25 hours and a settling at a new steady state by 90 hours.

Class 2: complex acute response

A total of 11 pathways within the pathway groups of amino acid metabolism[36,37] (arginine biosynthesis, biosynthesis of amino acids, and cysteine and methionine metabolism), carbohydrate metabolism[38,39] (pyruvate metabolism, carbon metabolism, glycolysis/gluconeogenesis, citrate cycle, and oxidative phosphorylation), regulation of essential organelles (ribosome and protein processing in endoplasmic reticulum),[41-43] and xenobiotic metabolism[44] (metabolism of xenobiotics by cytochrome P450) also report complex responses to acute MPL administration. In this class, the PAL responses captured indicate that some components (ie subgroups of genes) of pathways respond with monophasic behavior, whereas other components exhibit biphasic behavior. Acute MPL administration yields multiple profile patterns: both early and late phase of either monophasic or biphasic response. As previously defined, early monophasic response indicates DRN event peaks between 2 and 5 hours followed by a return to baseline between 18 and 30 hours. Late monophasic responses are defined by a DRN event peak between 7 and 15 hours followed by a return to baseline between 32 and 65 hours. Early biphasic responses are defined by a DRN event peak between 1 and 5 hours, an intermediate BS peak between 12 and 20 hours, and a return to baseline between 38 and 65 hours. Only one pathway exhibited a late biphasic response (arginine biosynthesis), defined by a DRN peak at 16 hours, and intermediate BS event peak at 23 hours and a return to baseline implied to occur after 72 hours.

Acute response: early monophasic and early biphasic. Pathways in this subgroup (protein processing in endoplasmic reticulum, metabolism of xenobiotics by cytochrome P450, and ribosome) exhibit both early monophasic and early biphasic responses to acute MPL administration. In response to chronic MPL administration, protein processing in endoplasmic reticulum exhibits both monophasic and biphasic responses. The chronic monophasic response exhibits a DRN event peak between 5 and 6 hours followed by a settling to a new steady state by 45 hours. The chronic biphasic response exhibits DRN event peak between 16 and 18 hours, an intermediate BS peak between 58 and 60 hours, and settles to a new steady state after 168 hours. The metabolism of xenobiotics by cytochrome P450 and ribosome pathways exhibit chronic biphasic behavior only. Metabolism of xenobiotics by cytochrome P450 reports DRN effect peaks between 2 and 4 hours, a peak due to the intermediate BS between 36 and 38 hours, and establishment of a new steady state is implied to occur after 168 hours. The ribosome pathways exhibits DRN effect peaks slightly later, between 16 and 29 hours, followed by intermediate BS effects between 58 and 60 hours, and establishment of a new steady state after 130 hours.

Acute response: early and late monophasic and early biphasic. Oxidative phosphorylation and carbon metabolism exhibit early and late monophasic, as well as early biphasic, responses to acute MPL administration. In response to chronic MPL administration, the oxidative phosphorylation pathway exhibits a monophasic response, exhibiting a steep incline until 40 hours with no clear event peak, but establishes a new steady state by 120 hours. Carbon metabolism exhibits both monophasic and biphasic responses to chronic MPL administration. Its chronic monophasic response reported a steep incline until 25 hours with no peak and establishes a new steady state by 30 hours. Its chronic biphasic response reports a DRN event peak between 5 and 9 hours, an intermediate BS peak between 35 and 40 hours, and a settling to a new steady state after 150 hours.

Acute response: late monophasic and early biphasic. Pathways cysteine and methionine metabolism, pyruvate metabolism, glycolysis/gluconeogenesis, biosynthesis of amino acids, and citrate cycle all exhibit this complex response to acute MPL administration, yielding both late monophasic and early biphasic responses. In response to chronic MPL administration, a combination of monophasic and biphasic responses is also observed. Cysteine and methionine metabolism reports chronic biphasic responses with DRN peaks between 2 and 9 hours, intermediate BS peaks between 28 and 30 hours, and establishment of a new steady state between 55 and 120 hours. Its chronic monophasic response exhibits a steep incline until 35 hours, no discernable peak, and establishment of a new steady state by 90 hours. Pyruvate metabolism exhibits a chronic monophasic response with a steep continuous incline, no peak, and an implication that the system will settle after 168 hours. Its chronic biphasic response exhibits a DRN event peak at 8 hours, an intermediate BS peak at 47 hours, and a new steady state is implied after 168 hours. Glycolysis/gluconeogenesis exhibits multiple chronic monophasic responses: one in which a peak is observed at 13 hours and a new steady state is achieved by 50 hours; as well as a monophasic response in which a steep incline is observed until 50 hours, no peak is identifiable, and a new steady state is implied to occur after 168 hours. Its biphasic response reports a DRN peak at 16 hours, an intermediate BS event peak at 57 hours, and establishment of a new steady state after 168 hours. Biosynthesis of amino acids pathway yields monophasic responses that exhibit DRN event peaks between 4 and 15 hours and settles to a new steady state between 35 and 45 hours. Biphasic responses to chronic MPL within this pathway report DRN event peaks between 9 and 15 hours, intermediate BS peaks between 27 and 45 hours, and settle to a new steady state by 80 to 120 hours. Chronic MPL administration exhibits citrate-cycle-only chronic biphasic response, reporting a DRN event peak between 9 and 13 hours, and intermediate BS peak between 32 and 37 hours, and establishment of a new steady state by 95 to 100 hours.

Acute response: late monophasic, early and late biphasic. Solely arginine biosynthesis demonstrates this combination of responses to acute MPL administration: late monophasic, as well as early and late biphasic. In response to chronic MPL, arginine biosynthesis exhibits monophasic behavior: exhibiting activities with steep and continuous inclines until 30 or 40 hours, no distinguishable peaks, and establishment of new steady states by 110 hours or after 168 hours.

Discussion

Synthetic GCs, such as MPL, are widely used anti-inflammatory drugs. Despite their widespread usage, the actions and secondary effects are still under investigation. Dosing regimens further complicate the host's response to the drug. Of importance is the liver response, being the organ of primary drug metabolism. Earlier studies have focused on liver-specific genome-wide transcriptomic analyses under acute and chronic dosing.[5,9–11,15,18,19,56–58,60–64] Transcriptional analyses focus on characterizing individual gene responses. Clustering and functional annotation enables a more complete characterization of the response. In this investigation, we approach the problem from another angle: we aim to characterize the dynamic response of functionally related a priori groupings of genes. We therefore aim to characterize the dynamic response of signaling and metabolic pathways following acute and chronic exposure to MPL. Characterizing the dynamics at the pathway level, or at the level of functionally related genes in general, enables comparison across platforms and experiments since the approach does not require consistency across experiments.

The first step of the analysis requires that we identify pathway appropriately represented in the microarray data. This is a critical step, as we need to confirm that pathways whose activities will be further analyzed are adequately represented in the experimental data. In doing so, we define fractional coverage (f_c) as the metric characterizing the extent to which a pathway is represented in the probe set used and reported in the genome-wide transcriptomic studies, as previously defined in the "Methods" section. We further assess the statistical significance of this metric by associating with the fractional coverage of a pathway with a p-value communicating our confidence that the fractional coverage is statistically significant. The metric is very important particularly in cases like the one we analyzed where we assess and compare experimental data using different platforms, or arrays as in our case. Since the initial set of genes whose activity is quantified are not the same across the two conditions (different animal studies make use of different microarrays), it is important to confirm that the pathways are appropriately represented because these pathways are identical across datasets and thus can be compared. As expected, as the statistical significance of the reliability of the fractional coverage metric is increased, the set of significantly represented pathways decreases. Our results indicate that of 209 pathways represented in KEGG which are relevant to *Rattus norvegicus* and the liver, 56 and 57 have statistically significant fractional coverage in the acute and chronic experiments, respectively, at a confidence level of 10^{-3}.

The next critical step is to associate a coherent dynamic response with each of the represented pathways. Our hypothesis is that each pathway is effectively a high-dimensional dynamic system, with each dimension corresponding to a gene in the pathway. We hypothesize that the multi-dimensional dynamics can be decomposed into intrinsic elements, identified via the SVD decomposition.[32,33,65] Singular value decomposition of the original data determined whether a pathway can generate at least one PAL, an indication that the pathway is active and should be further analyzed for multiple activity patterns in a manner that considers the inherent variability of the data. To account for the inherent variability in the experimental observations, the proposed bootstrap enabled us to identify likely intrinsic responses and further to assess a likelihood metric via corresponding p-values.

From within the sets of the 56 and 57 pathways identified to have statistically significant fractional coverage in the acute and chronic data, respectively, 26 pathways in the acute and 27 in the chronic yielded at least one significant PAL profile, indicating their significant pathway activity. Of these pathways, 24 are common to both the acute and chronic significant pathway sets (Table 3). The chronic pathways exhibit consistently higher fractional coverage than their acute counterparts. Completed a few years after the acute study, the chronic study had access to a microarray platform (230A) previously unavailable. Because both experiments investigate MPL within the liver, a consistent set of significant pathways is anticipated to emerge when comparing these data with our framework. However, it is likely that the difference in platform contributes to this discrepancy between acute and chronic pathway fractional coverage. The chronic study has a larger probe set on its microarray and thus has more genes to occupy each pathway. Thus, a consistent core set of pathways emerges as significantly represented and active in response to MPL in both datasets. These pathways emerge from the amino acid metabolism,[36,37] carbohydrate metabolism,[38,39] essential organelle regulation,[41–43] lipid metabolism,[34,35] metabolism of cofactors and vitamins,[40] and xenobiotic metabolism pathway families.[44]

Interestingly, the decomposition of the pathway dynamics to its intrinsic constituents verified that the emergent dynamics were consistent with likely mechanisms of regulation. Broadly, the intrinsic responses for the acute dosing reflects transient activity events due to DRN to GRE binding or transcription mediated via an intermediate BS influenced by MPL—while returning to baseline following the elimination of the drug. The chronic administration led to more complicated responses, including transient and persistent effects indicating both DRN to GRE binding or transcription mediated via intermediate BS. The bootstrapping step enabled us to investigate how the variability in a pathway dataset influences which PALs are dominant. The initial SVD step which determined whether a pathway can yield at least one PAL is a screening step which identifies if the pathway is at all active. The bootstrapping step is applied afterwards to ask the question, what kinds of significant activity emerge if the variability in the gene set is considered? For this investigation, this bootstrapping step is applied to pathways significant with p-values $\leq 10^{-3}$. It can be applied to pathway sets of any significance (ie pathway sets corresponding to p-value $\leq 10^{-1}$ and p-value $\leq 10^{-2}$); however, this is not necessary for our investigation as we are only interested in pathways that pass the screening SVD test at the greatest significance. This process identified pathways indicating consistent activity under either acute or chronic drug administration. The first important observation from our analysis is that, regardless of dosing, the pathways encapsulating the MPL effects are similar. Interestingly, chronic administration leads to the emergence of complex dynamics, not necessarily expected based on analysis of the acute response.

To systematically compare across dosing regimens and time horizons (72 hours in acute study and 168 hours in chronic study), we compare the intrinsic dynamics in the space of regulatory models. We hypothesize that each intrinsic response can be represented by corresponding PKPD models. Following the regulatory mechanisms proposed in previous publications,[18,56,57] we develop a two-compartment PK model for both acute and chronic dosing (Figure 4) and hypothesized either monophasic (equation 13) or biphasic (equations 14 and 15) regulation of the intrinsic component of the activity of the pathway. We therefore extend the concept of PD dynamic to characterizing the intrinsic responses at the pathway level. Our analysis indicates that the acute response initiates pathway dynamics consistent with the nature of the acute dosing: as MPL half-life of

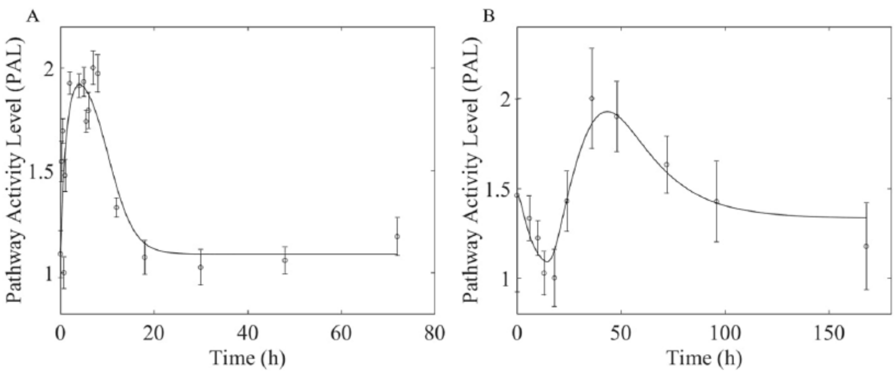

Figure 5. (A) Tryptophan metabolism pathway response to (A) acute and (B) chronic MPL administration. Example of Class 1 pathway which yields monophasic response to acute MPL administration but varies in its response to chronic MPL administration. The tryptophan metabolism pathway yields a biphasic response to chronic MPL administration indicating an increased complexity across dosing studies.

0.33 hours in ADX rats with a total drug clearance observed in ADX rats by 4.6 hours.[59]

We observed that the pathway responses emerging under acute dosing reflect monophasic or biphasic responses. However, the same pathway can lead to rather complicated dynamics under chronic administration. For consistency in our analysis, we examined pathways based on their response under acute administration. We, therefore, broadly identified two major categories: Class 1—capturing pathways yielding strictly monophasic response or strictly biphasic response to acute MPL administration; Class 2—reporting pathways yielding both monophasic and biphasic response to acute MPL administration. Within these categories (Table 4), pathway response to chronic MPL administration is compared.

Although PAL profiles resemble gene expression profiles, the features in these profiles do not necessarily correspond to up or down gene expression. The SVD linear combination technique preserves the relative magnitudes of gene expression profiles, but it does not preserve sign. For example, many genes which report an early upregulation event in their expression profiles will contribute to a single unique PAL, which will contain an early event peak. This is because the PAL is a linear combination of those gene expression profiles. A set of gene expression profiles will "resolve" to a PAL with the same timing and relative magnitude of features, but which may appear as a reflection of the gene expression profiles. What is critical to our analysis is the timing and relative magnitude of the peak events, which SVD preserves. These features determine whether a monophasic of biphasic mechanism is proposed.

Class 1 includes pathways exhibiting exclusively monophasic or exclusive biphasic regulation under acute dosing. Methylprednisolone induces a response which dies out as the drug is eventually eliminated from the system. Out of the 24 pathways, 13 pathways (tryptophan metabolism; beta-alanine metabolism; glutathione metabolism; proteasome; retinol metabolism; valine, leucine, and isoleucine degradation; propanoate metabolism; peroxisome; fatty acid degradation; steroid hormone biosynthesis; fatty acid metabolism; PPAR signaling pathway; and glyoxylate and dicarboxylate metabolism) exhibited this response under acute dosing. Almost all of these pathways reported early acute monophasic response. Only proteasome exhibited both early and late acute monophasic responses and only glyoxylate and dicarboxylate metabolism exhibited biphasic response to acute MPL. Interestingly, the chronic response for the Class 1 pathways manifested itself in multiple ways. Some pathways (valine, leucine, and isoleucine degradation; tryptophan metabolism; propanoate metabolism; peroxisome; fatty acid degradation; steroid hormone biosynthesis; fatty acid metabolism; and PPAR signaling pathway) exhibited strictly early monophasic response but increased complexity in response to chronic MPL administration, exhibiting both monophasic and biphasic responses in different subcomponents of each pathway. Tryptophan metabolism (Figure 5), a pathway describing the processing of the amino acid tryptophan into biproducts catabolized by glycolysis, and other energy regulating pathways,[37,66] exemplifies the observed shift from acute monophasic response to a response of greater complexity, such as chronic biphasic. This shift indicates that the mechanism of regulation presumed appropriate for describing the pathway's response to acute MPL administration is insufficient for describing the pathway's actual mechanism of regulation, which is revealed with greater complexity in its biphasic response to chronic MPL administration. The peroxisome pathway (Figure 6), which describes the biogenesis of peroxisome organelles and is crucial to redox signaling and lipid homeostasis,[34,43,66] yields strictly an acute monophasic response to acute MPL. However, the pathway reports multiple dominant activity patterns in response to chronic MPL. Pathway activity level profiles are linear combinations of the expression patterns of individual genes and if a pathway yields multiple significant PAL, it indicates that unique subgroups of genes within that pathway are responsible for each. The peroxisome pathway demonstrates this segregation of the pathway; within the gene set that composes the peroxisome pathway, unique subgroups of genes behave differently, some prescribing to monophasic regulation and yielding a chronic monophasic response (Figure 6B) and some prescribing to a

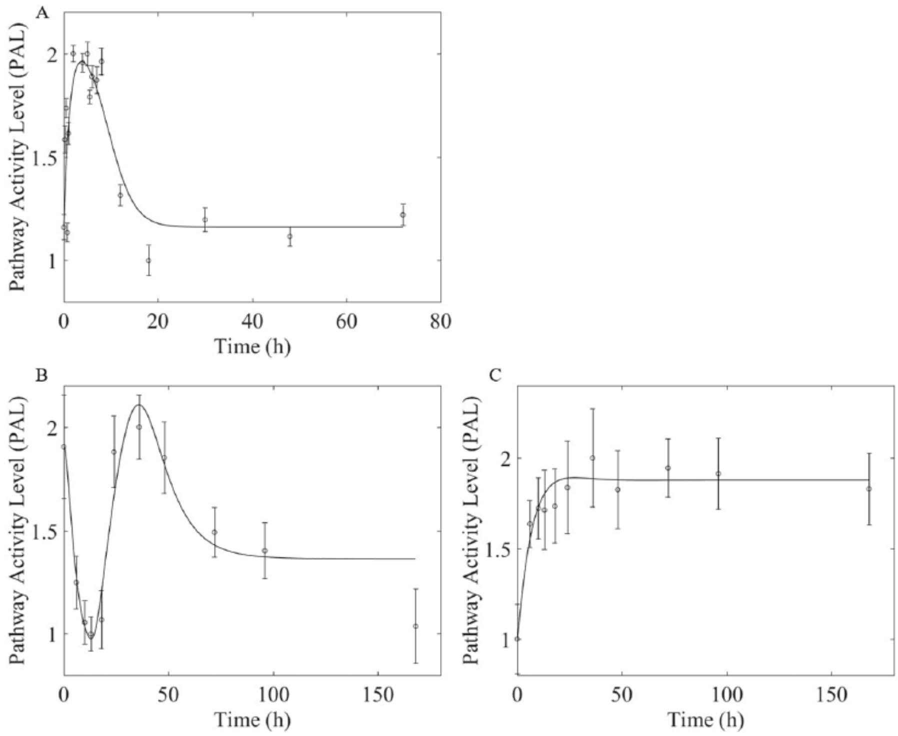

Figure 6. Peroxisome pathway response to (A) acute and (B, C) chronic MPL administration. Example of Class 1 pathway which yields monophasic response to acute MPL administration but varies in its response to chronic MPL administration. The peroxisome pathway yields both monophasic and biphasic responses to chronic MPL administration indicating an increased complexity across dosing studies as well as an internal complexity to the pathway. This pathway exhibits multiple dominant patterns of activity, each corresponding to unique subgroups of genes within the pathway.

chronic biphasic response (Figure 6C). Thus, the peroxisome pathway cannot be assumed homogeneous, and in fact represents at least two subgroups of uniquely regulated gene sets. Other pathways maintained a strictly monophasic response (beta-alanine metabolism, glutathione metabolism, proteasome, and retinol metabolism) to both acute and chronic MPL administration.

One pathway exhibited exclusively biphasic response to acute MPL, the glyoxylate and dicarboxylate metabolism pathway. This pathway describes energy regulating biosynthesis reactions for synthesis of carbohydrates from acetyl-CoA and fatty acids.[66] It yielded early biphasic response to acute MPL administration but a prolonged monophasic response to chronic MPL administration.

The 11 pathways that yielded more complex acute responses were included within Class 2. Some pathways (cysteine and methionine metabolism, glycolysis/gluconeogenesis, and carbon metabolism) within this class remained complex between dosing regimens, exhibiting both monophasic and biphasic behavior in different subcomponents of the pathway, in response to both acute and chronic MPL administration. The cysteine and methionine metabolism pathway (Figure 7) describes the metabolism of the eponymous amino acids into intermediates supplied to such processes as pyruvate metabolism and amino acid synthesizing pathways including valine, leucine, and isoleucine biosynthesis pathway.[36,37,66] It exemplifies the conservation of complex response between acute and chronic dosing. Regardless of dosing type, this pathway contains unique subgroups of genes whose expression patterns are the foundation for the PAL profiles observed in the pathway's response. A complexity which indicates that multiple mechanisms of regulation are required to describe the activity of this pathway. Other pathways shifted their response, exhibiting complex acute behavior but resolving to either strictly chronic monophasic behavior (arginine biosynthesis and oxidative phosphorylation) or strictly chronic biphasic behavior (protein processing in endoplasmic reticulum, citrate cycle [TCA cycle], pyruvate metabolism, metabolism of xenobiotics by cytochrome P450, and ribosome). The arginine biosynthesis pathway describes the construction of the amino acid arginine as well as the overlap of this process with others including the citrate cycle (catabolism of 2-oxoglutarate and production of fumarate), as well as the urea cycle (various steps including the generation of urea).[66] Acute MPL administration provokes both acute monophasic and acute biphasic responses, indicating that the pathway can be decomposed into uniquely regulated subcomponents of genes (Figure 8A and B). However, this behavior resolves to a strictly monophasic response to chronic MPL administration (Figure 8C). This observation indicates that some regulatory structures within this pathway may be overwhelmed by chronic MPL administration and lose the phenotypes that distinguish monophasic from biphasic mechanisms.

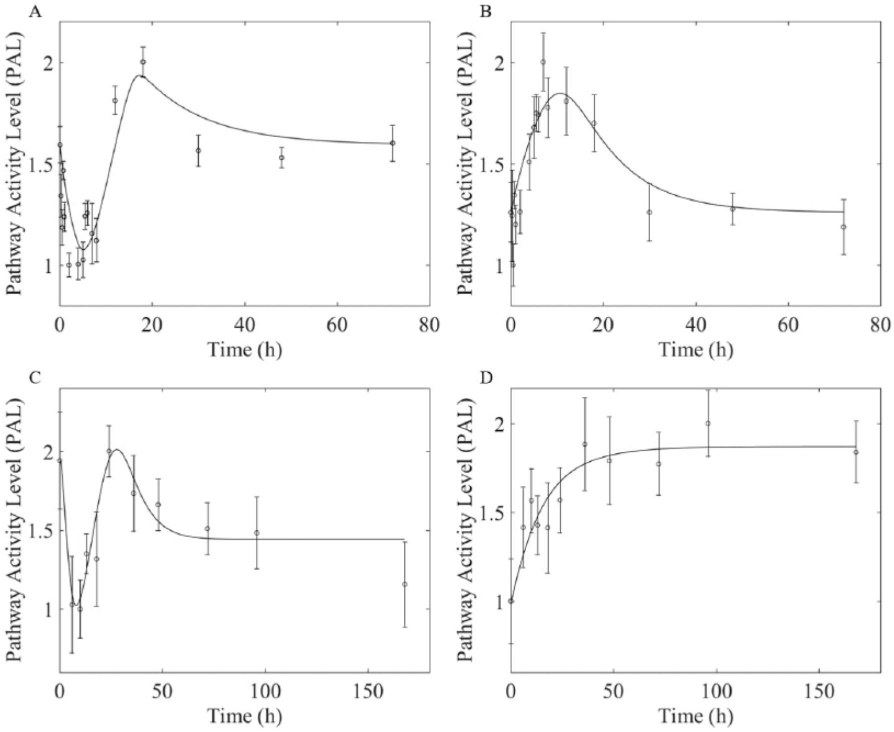

Figure 7. Cysteine and methionine metabolism pathway response to (A, B) acute and (C, D) chronic MPL administration. Example of Class 2 pathway which yields both monophasic and biphasic responses to acute MPL administration. This complexity indicates that multiple subgroups of genes within this pathway are regulated by different mechanisms. For the cysteine and methionine pathway, this complexity is preserved across dosing types.

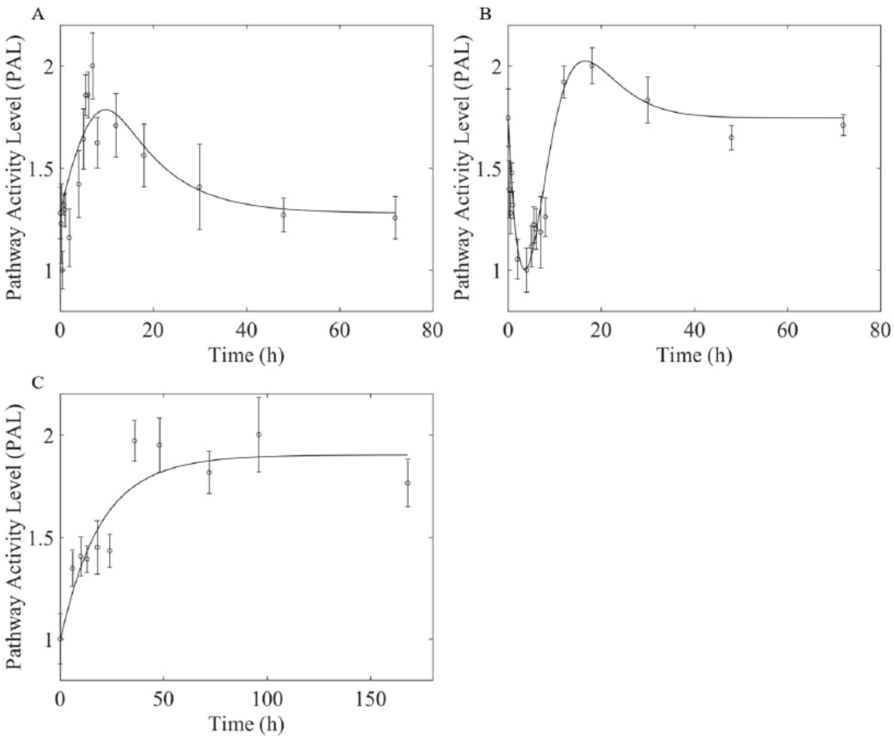

Figure 8. Arginine biosynthesis pathway response to (A, B) acute and (C) chronic MPL administration. Example of Class 2 pathway type which yields both monophasic and biphasic responses to acute MPL administration. This complexity indicates that multiple subgroups of genes within this pathway are regulated by different mechanisms. For the arginine biosynthesis pathway, chronic MPL administration yields a shift to a monophasic response.

Pathway responses from the remaining pathways within Table 4 are presented in the Supplemental Materials.

These results indicate that 16 of the 24 significant pathways exhibited a response pattern that changed between acute and chronic dosing. Of the 24 pathways, 8 (tryptophan metabolism; valine, leucine, and isoleucine degradation; propanoate metabolism; peroxisome; fatty acid degradation; steroid hormone biosynthesis; fatty acid metabolism; and PPAR signaling pathway) exhibit singularly monophasic or biphasic response to acute MPL administration but increase their complexity, exhibiting both monophasic and biphasic behavior, in response to chronic MPL administration. Increasing complexity indicates that a pathway's response to MPL is dosing specific, and that different subcomponents (unique groups of genes within a pathway) exhibit purely DRN binding to GRE regulation, whereas other components exhibit both DRN to GRE binding and transcription regulation mediated by an intermediate BS. The pathway cannot be defined by simply one response type. For some pathways, the response does not change with changing dosing.

Of the 24 pathways, 9 (beta-alanine metabolism, glutathione metabolism, proteasome, retinol metabolism, biosynthesis of amino acids, cysteine and methionine metabolism, glycolysis/gluconeogenesis, carbon metabolism, and protein processing in endoplasmic reticulum) exhibit no change in their dynamics, remaining monophasic in response to both dosing types or remaining chronic in response to both dosing types. This pathway's mechanism is sufficiently described by either strictly monophasic (DRN- to GRE-binding-regulated transcription) or biphasic (DRN- to GRE-binding-regulated transcription and MPL-influenced intermediate BS-mediating regulation of transcription); 4 pathways (citrate cycle, pyruvate metabolism, ribosome, and metabolism of xenobiotics by cytochrome P450) shift from a complex acute response to chronic biphasic behavior; and 3 pathways (glyoxylate and dicarboxylate metabolism, arginine biosynthesis, and oxidative phosphorylation) reduce from complex acute behavior to monophasic behavior in response to chronic MPL. This reduction in complexity may indicate a dosing dependence in which a system is overwhelmed by a particular magnitude of drug concentration. One mechanism may dominate in response to constant MPL administration.

The pathways that emerged within these classes exist within specific pathway families. Each of the pathways within the lipid metabolism[34] family (fatty acid degradation, steroid hormone biosynthesis, fatty acid metabolism, and PPAR signaling pathway) increased in complexity from acute monophasic to complex chronic responses. The amino acid metabolism[36,37] family yielded three pathways that increased in complexity from either monophasic or biphasic acute response to complex chronic response (tryptophan metabolism; valine, leucine, and isoleucine degradation; and biosynthesis of amino acids), three pathways that maintained either a monophasic response or a complex response to both dosing types (beta-alanine metabolism, glutathione metabolism, and cysteine and methionine metabolism), and one pathway that shifted from a complex acute response to a singularly monophasic response (arginine biosynthesis). Within the regulation of the essential organelles family, one pathway (peroxisome) increased in complexity from acute monophasic to complex chronic response, two pathways maintained the same response across dosing types either both monophasic or both complex (proteasome and protein processing in endoplasmic reticulum), and one pathway shifted from a complex acute response to a chronic biphasic response (ribosome). The retinol metabolism pathway within metabolism of cofactors and vitamins maintained the same monophasic response to acute and chronic MPL. The metabolism of xenobiotics by cytochrome P450 pathway within the xenobiotic metabolism family shifted from complex acute response to chronic biphasic.

This investigation uses meta-analysis technique to capture and compare physiological dynamics at the pathway level. This method provides a more comprehensive survey of physiological activity than do strictly gene-centric approaches, while capable of predicting likely regulatory structures. Designed to facilitate comparison of experiments that differ in platform, time scale, and dosing, this framework enabled a multiple dosing to identify and compare the influence of MPL within the liver. Significant influence of MPL is observed within six pathway families: amino acid metabolism,[36,37] carbohydrate metabolism,[38,39] regulation of essential organelles,[41-43] lipid metabolism,[34,35] metabolism of cofactors and vitamins,[40] and xenobiotic metabolism.[44] Within each family, most pathways demonstrate changed dynamics across dosing regimens. Furthermore, all pathways exhibit some form of dosing dependence easily identified when comparing acute to chronic responses within a pathway. Deconstruction of the activity of a pathway using SVD reveals multiple, temporally related, and co-dominant patterns of activity for each pathway, activity patterns which correspond to unique subcomponents within a pathway. Thus, this investigation not only identifies pathways with physiological relevance to the liver and MPL but also provides a complex, but defined, systemic characterization of the consequences of MPL within the liver and the possible regulatory structures that govern these pathways.

Author Contributions

AA, AB: performed calculations, conducted analyses, developed and edited the manuscript. AB: performed calculations. DD, RA, and WJ: edited the manuscript. IPA: conceived the studies and developed the manuscript.

Supplemental material

Supplemental material for this article is available online.

References

1. Barnes PJ. Anti-inflammatory actions of glucocorticoids: molecular mechanisms. *Clin Sci (Lond)*. 1998;94:557–572.
2. Swartz SL, Dluhy RG. Corticosteroids: clinical pharmacology and therapeutic use. *Drugs*. 1978;16:238–255.

3. Schaaf MJ, Cidlowski JA. Molecular mechanisms of glucocorticoid action and resistance. *J Steroid Biochem Mol Biol*. 2002;83:37–48.
4. Almon RR, Dubois DC, Jin JY, Jusko WJ. Temporal profiling of the transcriptional basis for the development of corticosteroid-induced insulin resistance in rat muscle. *J Endocrinol*. 2005;184:219–232.
5. Almon RR, DuBois DC, Jusko WJ. A microarray analysis of the temporal response of liver to methylprednisolone: a comparative analysis of two dosing regimens. *Endocrinology*. 2007;148:2209–2225.
6. Almon RR, DuBois DC, Piel WH, Jusko WJ. The genomic response of skeletal muscle to methylprednisolone using microarrays: tailoring data mining to the structure of the pharmacogenomic time series. *Pharmacogenomics*. 2004;5: 525–552.
7. Almon RR, Lai W, DuBois DC, Jusko WJ. Corticosteroid-regulated genes in rat kidney: mining time series array data. *Am J Physiol Endocrinol Metab*. 2005;289:E870–E882.
8. Almon RR, Yang E, Lai W, et al. Relationships between circadian rhythms and modulation of gene expression by glucocorticoids in skeletal muscle. *Am J Physiol Regul Integr Comp Physiol*. 2008;295:R1031–R1047.
9. Nguyen TT, Almon RR, Dubois DC, Jusko WJ, Androulakis IP. Comparative analysis of acute and chronic corticosteroid pharmacogenomic effects in rat liver: transcriptional dynamics and regulatory structures. *BMC Bioinformatics*. 2010;11:515.
10. Nguyen TT, Almon RR, Dubois DC, Sukumaran S, Jusko WJ, Androulakis IP. Tissue-specific gene expression and regulation in liver and muscle following chronic corticosteroid administration. *Gene Regul Syst Bio*. 2014;8:75–87.
11. Yang E, Almon RR, Dubois DC, Jusko WJ, Androulakis IP. Extracting global system dynamics of corticosteroid genomic effects in rat liver. *J Pharmacol Exp Ther*. 2008;324:1243–1254.
12. Yang EH, Almon RR, Dubois DC, Jusko WJ, Androulakis IP. Identification of global transcriptional dynamics. *PLoS ONE*. 2009;4:e5992.
13. Morand EF, Leech M. Glucocorticoid regulation of inflammation: the plot thickens. *Inflamm Res*. 1999;48:557–560.
14. Andrews RC, Walker BR. Glucocorticoids and insulin resistance: old hormones, new targets. *Clin Sci (Lond)*. 1999;96:513–523.
15. Almon RR, Dubois DC, Jin JY, Jusko WJ. Pharmacogenomic responses of rat liver to methylprednisolone: an approach to mining a rich microarray time series. *AAPS J*. 2005;7:E156–E194.
16. Almon RR, DuBois DC, Yao Z, Hoffman EP, Ghimbovschi S, Jusko WJ. Microarray analysis of the temporal response of skeletal muscle to methylprednisolone: comparative analysis of two dosing regimens. *Physiol Genomics*. 2007;30:282–299.
17. Yao Z, Hoffman EP, Ghimbovschi S, Dubois DC, Almon RR, Jusko WJ. Mathematical modeling of corticosteroid pharmacogenomics in rat muscle following acute and chronic methylprednisolone dosing. *Mol Pharm*. 2008;5:328–339.
18. Hazra A, DuBois DC, Almon RR, Snyder GH, Jusko WJ. Pharmacodynamic modeling of acute and chronic effects of methylprednisolone on hepatic urea cycle genes in rats. *Gene Regul Syst Bio*. 2008;2:1–19.
19. Jin JY, Almon RR, DuBois DC, Jusko WJ. Modeling of corticosteroid pharmacogenomics in rat liver using gene microarrays. *J Pharmacol Exp Ther*. 2003;307:93–109.
20. Jiang H, Deng Y, Chen HS, et al. Joint analysis of two microarray gene-expression data sets to select lung adenocarcinoma marker genes. *BMC Bioinformatics*. 2004;5:81.
21. Kim KY, Ki DH, Jeong HJ, Jeung HC, Chung HC, Rha SY. Novel and simple transformation algorithm for combining microarray data sets. *BMC Bioinformatics*. 2007;8:218.
22. Park T, Yi SG, Shin YK, Lee S. Combining multiple microarrays in the presence of controlling variables. *Bioinformatics*. 2006;22:1682–1689.
23. Shabalin AA, Tjelmeland H, Fan C, Perou CM, Nobel AB. Merging two gene-expression studies via cross-platform normalization. *Bioinformatics*. 2008;24: 1154–1160.
24. Carter SL, Eklund AC, Mecham BH, Kohane IS, Szallasi Z. Redefinition of Affymetrix probe sets by sequence overlap with cDNA microarray probes reduces cross-platform inconsistencies in cancer-associated gene expression measurements. *BMC Bioinformatics*. 2005;6:107.
25. Lu J, Lee JC, Salit ML, Cam MC. Transcript-based redefinition of grouped oligonucleotide probe sets using AceView: high-resolution annotation for microarrays. *BMC Bioinformatics*. 2007;8:108.
26. Mecham BH, Klus GT, Strovel J, et al. Sequence-matched probes produce increased cross-platform consistency and more reproducible biological results in microarray-based gene expression measurements. *Nucleic Acids Res*. 2004;32:e74.
27. Morris JS, Wu C, Coombes KR, Baggerly KA, Wang J, Zhang L. Alternative probeset definitions for combining microarray data across studies using different versions of affymetrix oligonucleotide arrays. In: *Meta-Analysis in Genetics*. New York, NY: Chapman & Hall; 2006:1–21.
28. Ramasamy A, Mondry A, Holmes CC, Altman DG. Key issues in conducting a meta-analysis of gene expression microarray datasets. *PLoS Med*. 2008;5:e184.
29. Ghosh D, Barette TR, Rhodes D, Chinnaiyan AM. Statistical issues and methods for meta-analysis of microarray data: a case study in prostate cancer. *Funct Integr Genomics*. 2003;3:180–188.
30. Euling SY, White L, Ovacik AM, et al. An approach to using toxicogenomic data in risk assessment: dibutyl phthalate case study. *Environ Molec Mutagen*. 2011;52:S16.
31. Euling SY, White LD, Kim AS, et al. Use of genomic data in risk assessment case study: II. Evaluation of the dibutyl phthalate toxicogenomic data set. *Toxicol Appl Pharmacol*. 2013;271:349–362.
32. Ovacik MA, Sen B, Euling SY, Gaido KW, Ierapetritou MG, Androulakis IP. Pathway modeling of microarray data: a case study of pathway activity changes in the testis following in utero exposure to dibutyl phthalate (DBP). *Toxicol Appl Pharmacol*. 2013;271:386–394.
33. Ovacik MA, Sukumaran S, Almon RR, DuBois DC, Jusko WJ, Androulakis IP. Circadian signatures in rat liver: from gene expression to pathways. *BMC Bioinformatics*. 2010;11:540.
34. Peckett AJ, Wright DC, Riddell MC. The effects of glucocorticoids on adipose tissue lipid metabolism. *Metabolism*. 2011;60:1500–1510.
35. Macfarlane DP, Forbes S, Walker BR. Glucocorticoids and fatty acid metabolism in humans: fuelling fat redistribution in the metabolic syndrome. *J Endocrinol*. 2008;197:189–204.
36. Ratnam S, Maclean KN, Jacobs RL, Brosnan ME, Kraus JP, Brosnan JT. Hormonal regulation of cystathionine beta-synthase expression in liver. *J Biol Chem*. 2002;277:42912–42918.
37. Christiansen JJ, Djurhuus CB, Gravholt CH, et al. Effects of cortisol on carbohydrate, lipid, and protein metabolism: studies of acute cortisol withdrawal in adrenocortical failure. *J Clin Endocrinol Metab*. 2007;92:3553–3559.
38. McMahon M, Gerich J, Rizza R. Effects of glucocorticoids on carbohydrate metabolism. *Diabetes Metab Rev*. 1988;4:17–30.
39. Nader N, Ng SS, Wang Y, Abel BS, Chrousos GP, Kino T. Liver x receptors regulate the transcriptional activity of the glucocorticoid receptor: implications for the carbohydrate metabolism. *PLoS ONE*. 2012;7:e26751.
40. Pascussi JM, Drocourt L, Fabre JM, Maurel P, Vilarem MJ. Dexamethasone induces pregnane X receptor and retinoid X receptor-alpha expression in human hepatocytes: synergistic increase of CYP3A4 induction by pregnane X receptor activators. *Mol Pharmacol*. 2000;58:361–372.
41. Rhen T, Cidlowski JA. Anti-inflammatory action of glucocorticoids—new mechanisms for old drugs. *N Engl J Med*. 2005;353:1711–1723.
42. Wallace AD, Cidlowski JA. Proteasome-mediated glucocorticoid receptor degradation restricts transcriptional signaling by glucocorticoids. *J Biol Chem*. 2001;276:42714–42721.
43. Cuzzocrea S, Bruscoli S, Mazzon E, et al. Peroxisome proliferator-activated receptor-alpha contributes to the anti-inflammatory activity of glucocorticoids. *Mol Pharmacol*. 2008;73:323–337.
44. Dvorak Z, Pavek P. Regulation of drug-metabolizing cytochrome P450 enzymes by glucocorticoids. *Drug Metab Rev*. 2010;42:621–635.
45. Boudinot FD, D'Ambrosio R, Jusko WJ. Receptor-mediated pharmacodynamics of prednisolone in the rat. 1986;14:469–493.
46. Ballard PL, Baxter JD, Higgins SJ, Rousseau GG, Tomkins GM. General presence of glucocorticoid receptors in mammalian tissues. 1974;94: 998–1002.
47. Almon RR, Yang E, Lai W, Androulakis IP, DuBois DC, Jusko WJ. Circadian variations in rat liver gene expression: relationships to drug actions. *J Pharmacol Exp Ther*. 2008;326:700–716.
48. Ogata H, Goto S, Sato K, Fujibuchi W, Bono H, Kanehisa M. KEGG: Kyoto encyclopedia of genes and genomes. *Nucleic Acids Res*. 1999;27:29-34.
49. Kanehisa M. The KEGG database. *Novartis Found Symp*. 2002;247:91-101, discussion 101-103, 119-128, 244-252.
50. Huang da W, Sherman BT, Lempicki RA. Bioinformatics enrichment tools: paths toward the comprehensive functional analysis of large gene lists. *Nucleic Acids Res*. 2009;37:1–13.
51. Huang da W, Sherman BT, Lempicki RA. Systematic and integrative analysis of large gene lists using DAVID bioinformatics resources. *Nat Protoc*. 2009;4:44–57.
52. The UniProt Consortium T. UniProt: the universal protein knowledgebase. *Nucleic Acids Res*. 2018;46:2699.
53. Subramanian A, Tamayo P, Mootha VK, et al. Gene set enrichment analysis: a knowledge-based approach for interpreting genome-wide expression profiles. *Proc Natl Acad Sci U S A*. 2005;102:15545–15550.
54. Kallio A, Vuokko N, Ojala M, Haiminen N, Mannila H. Randomization techniques for assessing the significance of gene periodicity results. *BMC Bioinformatics*. 2011;12:330.
55. *MATLAB and Statistics Toolbox Release 2016B*. Natick, MA: The MathWorks, Inc; 2016.
56. Ramakrishnan R, DuBois DC, Almon RR, Pyszczynski NA, Jusko WJ. Fifth-generation model for corticosteroid pharmacodynamics: application to steady-state receptor down-regulation and enzyme induction patterns during seven-day continuous infusion of methylprednisolone in rats. *J Pharmacokinet Pharmacodyn*. 2002;29:1–24.
57. Sun YN, DuBois DC, Almon RR, Jusko WJ. Fourth-generation model for corticosteroid pharmacodynamics: a model for methylprednisolone effects on receptor

/gene-mediated glucocorticoid receptor down-regulation and tyrosine aminotransferase induction in rat liver. *J Pharmacokinet Biopharm*. 1998;26:289–317.
58. Ramakrishnan R, DuBois DC, Almon RR, Pyszczynski NA, Jusko WJ. Pharmacodynamics and pharmacogenomics of methylprednisolone during 7-day infusions in rats. *J Pharmacol Exp Ther*. 2002;300:245–256.
59. Hazra A, Pyszczynski N, DuBois DC, Almon RR, Jusko WJ. Pharmacokinetics of methylprednisolone after intravenous and intramuscular administration in rats. *Biopharm Drug Dispos*. 2007;28:263–273.
60. Almon RR, Yang E, Lai W, Androulakis IP, DuBois DC, Jusko WJ. Circadian variations in rat liver gene expression: Relationships to drug actions. *J Pharmacol Exp Ther*. 2008;326:700–716.
61. Ayyar VS, Almon RR, DuBois DC, Sukumaran S, Qu J, Jusko WJ. Functional proteomic analysis of corticosteroid pharmacodynamics in rat liver: relationship to hepatic stress, signaling, energy regulation, and drug metabolism. *J Proteomics*. 2017;160:84–105.
62. Kamisoglu K, Sukumaran S, Nouri-Nigjeh E, et al. Tandem analysis of transcriptome and proteome changes after a single dose of corticosteroid: a systems approach to liver function in pharmacogenomics. *OMICS*. 2015;19: 80–91.
63. Nguyen TT, Almon RR, DuBois DC, Jusko WJ, Androulakis IP. Importance of replication in analyzing time-series gene expression data: corticosteroid dynamics and circadian patterns in rat liver. *BMC Bioinformatics*. 2010;11:279.
64. Nouri-Nigjeh E, Sukumaran S, Tu C, et al. Highly multiplexed and reproducible ion-current-based strategy for large-scale quantitative proteomics and the application to protein expression dynamics induced by methylprednisolone in 60 rats. *Anal Chem*. 2014;86:8149–8157.
65. Tomfohr J, Lu J, Kepler TB. Pathway level analysis of gene expression using singular value decomposition. *BMC Bioinformatics*. 2005;6:225.
66. KEGG. *Kyoto Encyclopedia in Genes and Genomes (KEGG)*. Kyoto, Japan: Kanehisa Laboratories; 2017.